Chapter

Thin Film Stabilization of Different VO_2 Polymorphs

Manish Kumar, Chirag Saharan and Sunita Rani

Abstract

In recent years, VO_2 has emerged as a popular candidate among the scientific community across the globe owing to its unique technological and fundamental aspects. VO_2 can exist in several polymorphs (such as: A, B, C, D, M_1, M_2, M_3, P, R and T) which offer a broad spectrum of functionalities suitable for numerous potential applications likewise smart windows, switching devices, memory materials, battery materials and so on. Each phase of VO_2 has specific physical and chemical properties. The device realization based on specific functionality call for stabilization of good quality single phase VO_2 thin films of desired polymorphs. Hence, the control on the growth of different VO_2 polymorphs in thin film form is very crucial. Different polymorphs of VO_2 can be stabilized by selecting the growth route, growth parameters and type of substrate etc. In this chapter, we present an overview of stabilization of the different phases of VO_2 in the thin film form and the identification of these phases mainly by X-ray diffraction and Raman spectroscopy techniques.

Keywords: thin film, VO_2, thermochromic, X-ray diffraction, Raman

1. Introduction

Thin film materials with 'smart' properties have attracted increasing attention in past few decades, as we move towards the smarter world [1]. This is driven by the fact that these materials react to the variation in parameters such as temperature, pressure, electric or magnetic fields etc. [2–13]. Vanadium dioxide (VO_2) is a well-known 'smart material' which is popular since the Morin' work in 1959 [14]. Its monoclinic M1 phase exhibits a metal–insulator transition (MIT) near room temperature, accompanied by larges changes in the structural, electronic and optical properties [15]. These distinctive features makes it attractive in smart windows, switching devices, memory materials and so on [16–18]. Being a strongly correlated electron system, VO_2 is equally attractive to condensed-matter physicists [19–22].

VO_2 can exhibit various polymorphic structures (such as: A, B, C, D, M_1, M_2, M_3, P, R and T), each having quite different physical and chemical properties [23–31]. Among these polymorphs, many are neither stable in ambient conditions nor can be easily synthesized. This happens because vanadium oxides can adopt a wide range of V:O ratios, resulting in different structural motifs. Phase space diagram (**Figure 1**) for the vanadium oxides indicates that there are more than 15 other stable vanadium oxides phases (like VO, V_2O_3, V_3O_5 etc.) and only a narrow window in phase space exist in which the pure semiconducting phase of VO_2 can be grown [32]. This narrow window strongly limits the synthesis of VO_2 either in the form of bulk crystals, thin films, or micro- and nanostructures. Nonetheless, different stoichiometric

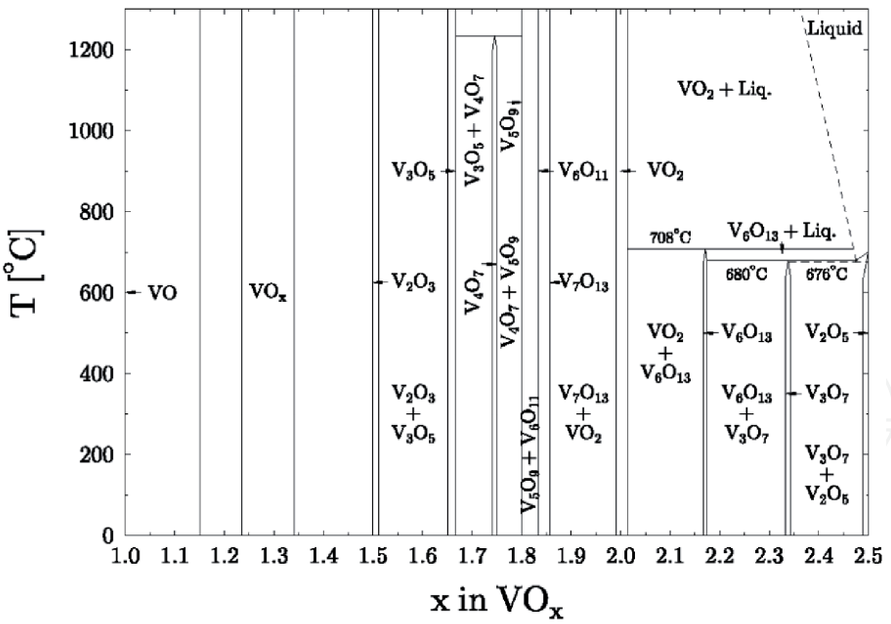

Figure 1.
Phase space diagram for the vanadium oxides. Note the narrow window within which stoichiometric VO_2 can be grown for x = 2.0 (reprinted from Ref. [32]).

Phase	Crystal structure (space group)	Lattice parameters				Comments and References
		a(Å)	*b*(Å)	*c*(Å)	*β*(°)	
VO_2 (A)	Tetragonal($P4_2/ncm$) (138)	8.43	8.43	7.68		[60]
VO_2 (B)	Monoclinic(C_2/m) (12)	12.03	3.69	6.42	106.6	[60]
VO_2 (C)	Tetragonal(I4/mnm) (139)	3.72	3.72	15.42		[24]
VO_2 (D)	Monoclinic(P2/c) (13)	4.59	5.68	4.91	89.3	[26]
VO_2 (P)	Orthorhombic(Pbnm) (62)	4.95	9.33	2.89		[28]
VO_2 (M_1)	Monoclinic($P2_1/c$) (14)	5.74	4.52	5.38	122.6	[61]
VO_2 (M_2)	Monoclinic(C2/m) (12)	9.08	5.76	4.53	91.3	[62]
VO_2 (M_3)	Monoclinic(P2/m) (10)	4.50	2.89	4.61	91.7	[62]
VO_2 (T)	Triclinic(P-1) (2)	9.06	5.77	4.52	91.4	[63]
VO_2 (R)	Tetragonal($P4_2/mnm$) (136)	4.55	4.55	2.86		[61]

Table 1.
The crystallography data for VO_2 polymorphs.

VO_2 polymorphs have been stabilized using techniques such as sputtering, pulsed laser deposition (PLD), sol–gel deposition, reactive evaporation and metal–organic chemical vapor deposition (MOCVD) etc. [15, 23, 25, 31, 33–38].

Koide and Takei appears to be the first to grow VO_2 thin films by chemical vapor deposition (CVD) technique in 1967 [39]. In their deposition method, fumes of vanadium oxychloride ($VOCl_3$) was carried by N_2 gas into the growth chamber and was hydrolyzed on the surface of rutile substrates to give epitaxial VO_2 films. In 1967, VO_2 thin films were also grown using reactive sputtering by Fuls et al. who made the films by reactive ion-beam sputtering of a vanadium target in an argon–oxygen atmosphere [40]. PLD emerged as a deposition technique for oxide superconductors in the late 1980s, and was first used to prepare VO_2 thin films by Borek et al. in 1993 [41]. Since then, consistent efforts have been made to grow thin films of various VO_2 polymorphs by using different deposition techniques/routes. Sputtering and PLD are the leading deposition techniques used to grow different VO_2 thin films polymorphs [42–46]. This is because of the ease with which one can play the deposition parameters in these techniques to stabilize thin films of various compounds [47–60].

In this chapter we will focus on the stabilization of thin film of six main VO_2 polymorphs: VO_2 (M_1), VO_2 (M_2), VO_2 (R), VO_2 (T), VO_2 (A) and VO_2 (B). But in passing it should be noted that VO_2 polymorphs likewise VO_2 (M_3), VO_2 (P), VO_2 (C) and VO_2 (D) have also been mostly studied in bulk and nanostructure form and reports are missing on thin film stabilization of these phases [24–29, 31]. Space group and lattice parameters of different VO_2 polymorphs known to us are tabulated in **Table 1**.

2. Thin film growth of different VO_2 polymorphs

2.1 VO_2 (M_1) and VO_2 (R) phase thin films

Monoclinic VO_2 (M_1) (a = 5.74 Å, b = 4.52 Å, c = 5.38 Å, β = 122.6°) with space group $P2_1/c$ is the most widely studied inorganic thermochromic material which is an insulator at room temperature. It shows a first-order MIT at 68°C with a concomitant structural transition into rutile tetragonal VO_2 (R) (a = b = 4.55 Å, c = 2.86 Å) having space group $P4_2/mnm$ [61]. Because of MIT and the associated huge changes in the structural, electronic and optical properties, VO_2 (M_1) and VO_2 (R) are attractive for applications in smart windows, switching devices, memory materials and so on [16, 17].

Figure 2 shows the structural arrangement of four different phases of VO_2 [64]. In the VO_2 (R) phase, the vanadium atoms are equally spaced along the rutile c axis (c_R), while in the VO_2 (M_1) phase, simultaneous dimerization and tilting in equivalent chains occur, leading to a zigzag pattern.

Highly oriented VO_2 (M_1) thin films on R-cut sapphire substrate were prepared by Borek et al. using PLD [41]. They ablated metallic vanadium target by a KrF pulsed excimer laser in an ultrahigh vacuum deposition chamber with Ar and O_2 (10:1) atmosphere of 100–200 mTorr, and a substrate temperature (T_s) ~ 500°C followed by 1 hour post deposition annealing in the same environment. Since then PLD was employed by number of groups to grow good quality VO_2 (M_1) thin films by varying the deposition parameters and post deposition treatment [44–46, 65]. Several other techniques such as sputtering, CVD, etc. were also employed to grow polycrystalline and epitaxial VO_2 (M_1) thin films on various substrates of different orientation [34, 42, 43, 66–69]. To date, most VO_2 (M_1) films have been grown on substrates such as sapphire (c-type, m-type, r-type and a-type), TiO_2, perovskite oxides, Si and Quartz. **Figure 3(a)** shows the grazing incidence X-ray diffraction (GIXRD) data of polycrystalline VO_2 (M_1) thin film by Kumar et al. which was

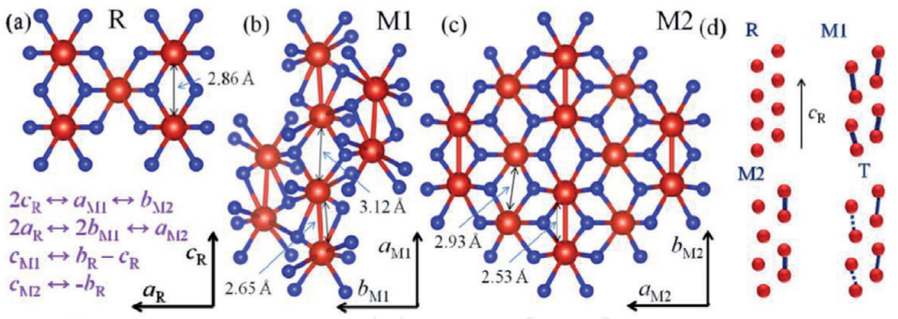

Figure 2.
The schematic structures for (a) rutile (R), (b) monoclinic M_1, and (c) M_2 phases of VO_2. Red and blue balls denote vanadium and oxygen atoms, respectively. (d) The arrangement of vanadium chains in the four phases without oxygen atoms (a-d reprinted from Ref. [64]).

grown on quartz substrate by sputtering VO_2 at room temperature and post deposition annealing at 500°C [69]. **Figure 3(b)–d** depict the X-ray diffraction (XRD) patterns of VO_2 (M1) thin film grown on TiO_2 and Al_2O_3 substrates of different orientation [46, 70].

VO_2 (R) is the high temperature phase of VO_2 (M_1). So, VO_2 (M_1) thin films generally transforms to VO_2 (R) phase when heated above the MIT temperature. Apart from this, thin films showing VO_2 (R) phase at room temperature can also be stabilized by strain, hydrogenation, oxygen vacancies and doping etc. [71–76]. Fan et al. reported the growth of ultrathin VO_2 (R) phase thin film on TiO_2 (002) substrate [71]. Y. Zhao et al. showed that hydrogenation can also lead to growth of VO_2 (R) phase thin film [72]. Very recently, Liang et al. described that increase in concentration of W dopant in $V_{1-x}W_xO_2$/Si thin films favors the growth of VO_2 (R) phase [73]. **Figure 4** shows the XRD patterns of VO_2 (R) phase thin films grown by different groups.

2.2 VO_2 (T) phase and VO_2 (M_2) phase thin films

VO_2 (T) phase and VO_2 (M_2) are known to be Mott-Hubbard type insulator which may find use in Mottronics and novel electronic transport applications [15, 18]. These phases are structurally different from VO_2 (M_1) and VO_2 (R) phase because of dissimilar types of vanadium chains and dimerization as shown in **Figure 2**. VO_2 (M_2) phase contains two distinct types of vanadium chains: one half of the vanadium atoms pair but do not tilt, while the other half are equidistant which tilts but do not pair. Triclinic phase i.e. VO_2 (T) phase can be thought of as an intermediate phase between VO_2 (M_1) and VO_2 (M_2) phases, having two types of inequivalent vanadium chains (or sublattices) in which the vanadium atoms are paired and tilted to different degrees. VO_2 (T) phase and VO_2 (M_2) are not as stable phase as VO_2 (M_1) and VO_2 (R). But, doping and/or strain can stabilize these phases [15, 35, 77]. Strelcov et al. presented a phase diagram which demonstrate the influence of chemical doping and uniaxial stress on the phase structure of VO_2 [35]. This phase diagram (**Figure 5(a)**) indicates that either of M_1, M_2, T, or R phase of VO_2 can exist depending on the type of dopant and/or stress. Majid et al. reported the Cr doping driven growth of VO_2 (T) phase thin films [15]. **Figure 5(b)** shows their XRD pattern of grown VO_2 (M_1) and VO_2 (T) phase thin films. Stress-induced VO_2 films with M_2 monoclinic phase stable at room temperature; were grown by Okimura et al. using inductively coupled plasma-assisted (ICP) reactive sputtering technique with various rf power fed to the coil for ICP (**Figure 5(c)**) at constant Ts of 450°C and at varying Ts, under constant rf power (**Figure 5(d)**) [77]. Apart from this work, there are not much reports on the growth of single phase VO_2 (M_2) thin films which are stable at room temperature. But, there are numerous reports on the evolution of intermediate M_2 phase in VO_2 thin films

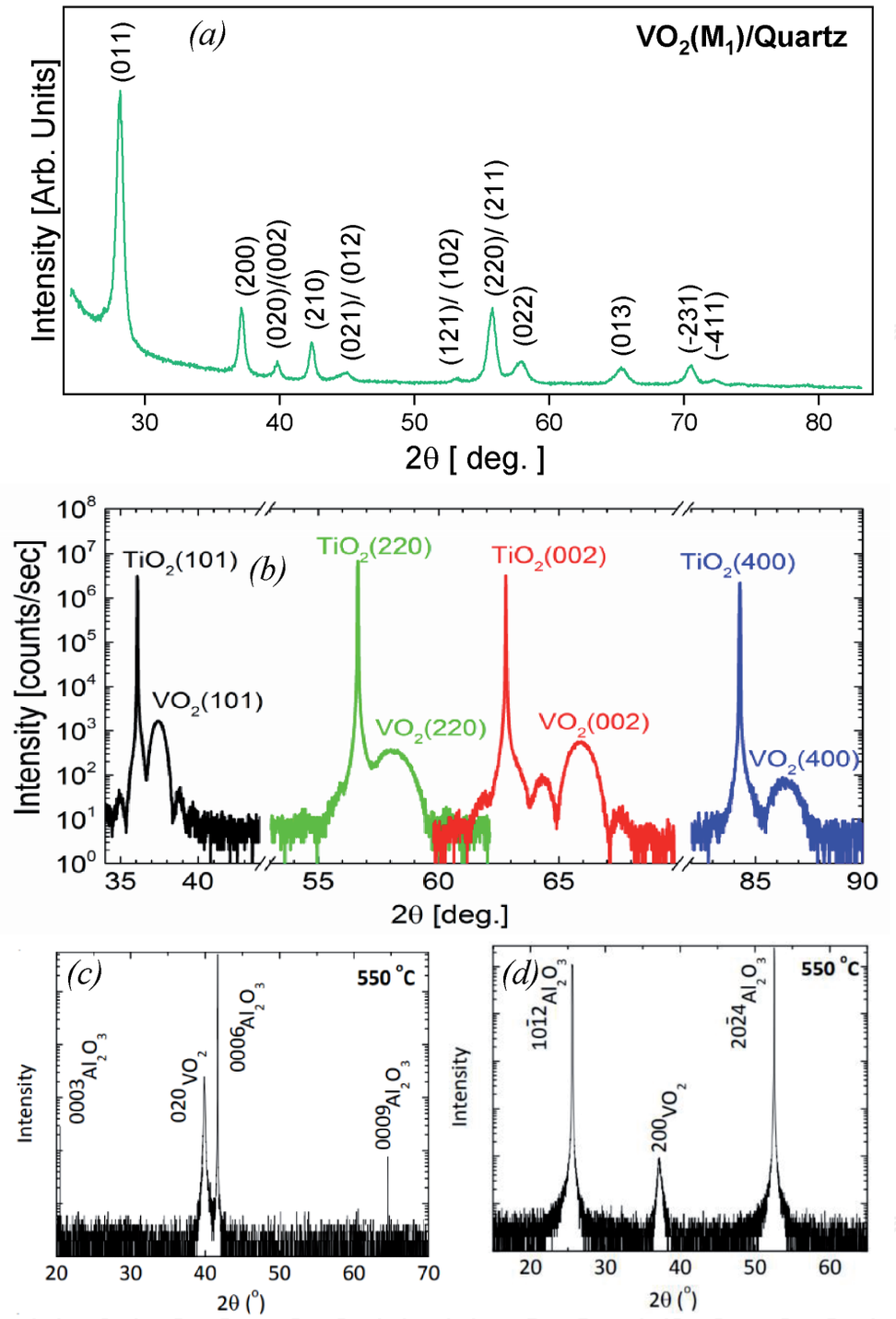

Figure 3.
(a) GIXRD data of VO_2 (M1) thin film prepared on quartz substrate [69]. XRD data of epitaxial VO_2 (M1) thin films grown on (b) TiO_2 substrates of different orientation (reprinted from Ref. [46]), (c) c-cut sapphire and (d) r-cut sapphire (c, d adopted from Ref. [70]).

during the monoclinic M_1 to rutile R transition [15, 69, 78–81]. This intermediate M2 phase in VO_2 thin film can be introduced by selecting the particular substrate temperature, doping, thickness etc. Kumar et al. witnessed the intermediate M2 phase temperature dependent XRD measurements across the MIT transition in polycrystalline VO_2 thin films grown on quartz substrate using sputtering technique followed by rapid thermal annealing at 530°C (**Figure 6(b)**) [69]. However, they have not observed the intermediate M_2 phase for films annealed at 500°C (**Figure 6(a)**). Majid et al. noticed the evolution of intermediate M_2 phase in temperature dependent Raman measurements of Cr doped VO_2 thin films during T ➔ R phase transition (**Figure 6(d)**) [15]. For undoped VO_2 thin films normal M_1➔R phase transition crossover was observed

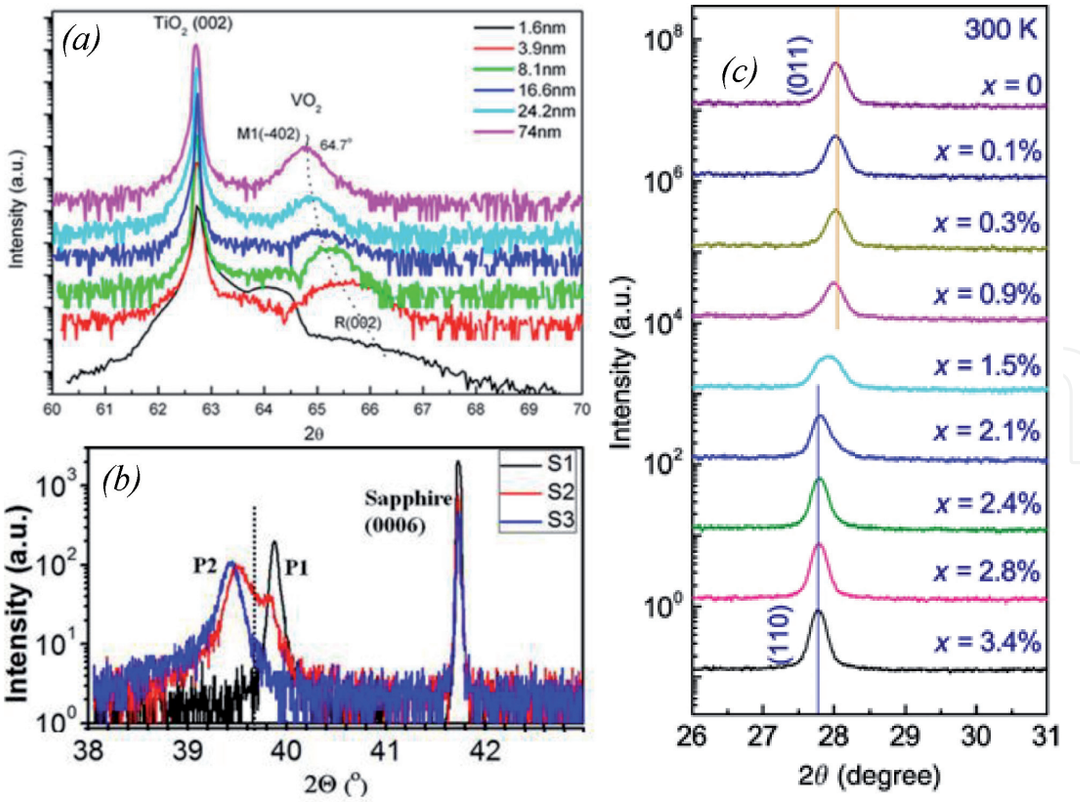

Figure 4.
(a) XRD profiles for thickness-dependence VO_2 films on TiO_2 substrate [Reprinted with permission from Fan et al [71]. Copyright (2014) American Chemical Society]. (b) XRD of pure (M_1 phase) and hydrogen-doping stabilized metallic (R phase) VO_2 thin films prepared on sapphire substrate (Reprinted from Ref. [72], with the permission of AIP Publishing). (c) Room temperature XRD of different $V_{1-x}W_xO_2$/Si thin films (adopted from Ref. [73]).

without signatures of intermediate M_2 phase °C (**Figure 6(c)**). Ji et al. stressed the role of microstructure on the M_1-M_2 phase transition in epitaxial VO_2 thin films of different thicknesses [78]. Their temperature dependent Raman measurement result on 90 nm and 150 nm thick VO_2 thin film sample are depicted in **Figure 6(e)** and **(f)** respectively. Azhan et al. also found intermediate M_2 phase in VO_2 thin films with large crystalline domains [79].

2.3 VO_2 (A) and VO_2 (B) phase thin films

The layered polymorphs VO_2 (A) and VO_2 (B) are important materials from science and technology perspective. VO_2 (B) has been long considered as a promising electrode material for Li ion batteries since the after report of Li et al. in 1994 [82]. It emerged as a promising cathode material owing to its layered structure and outstanding electrochemical performance [83, 84]. Also, it is important for the study of strong electronic correlations resulting from structure. On the other hand, VO_2 (A) phase is highly metastable and therefore the physical properties and the potential for technical applications have not been explored in detail. This phase is an intermediate phase between VO_2 (B) and VO_2 (R), and has a reversible phase transition at ~162°C [85, 86]. The crystal structure of VO_2 (A) and VO_2 (B) phase with possible epitaxial relation on $SrTiO_3$ substrate, are illustrated in **Figure 7(a)** and **(b)** respectively [23]. At room temperature, the metastable monoclinic VO_2 (B) adopts a structure derived from V_2O_5 and belongs to space group C2/m while VO_2 (A) adopts a tetragonal unit cell with a space group $P4_2/ncm$ [23]. Growth of single crystalline VO_2 (B) is very challenging due to the complex crystal structure. Similarly to VO_2 (B), the study of VO_2 (A) has so far been limited.

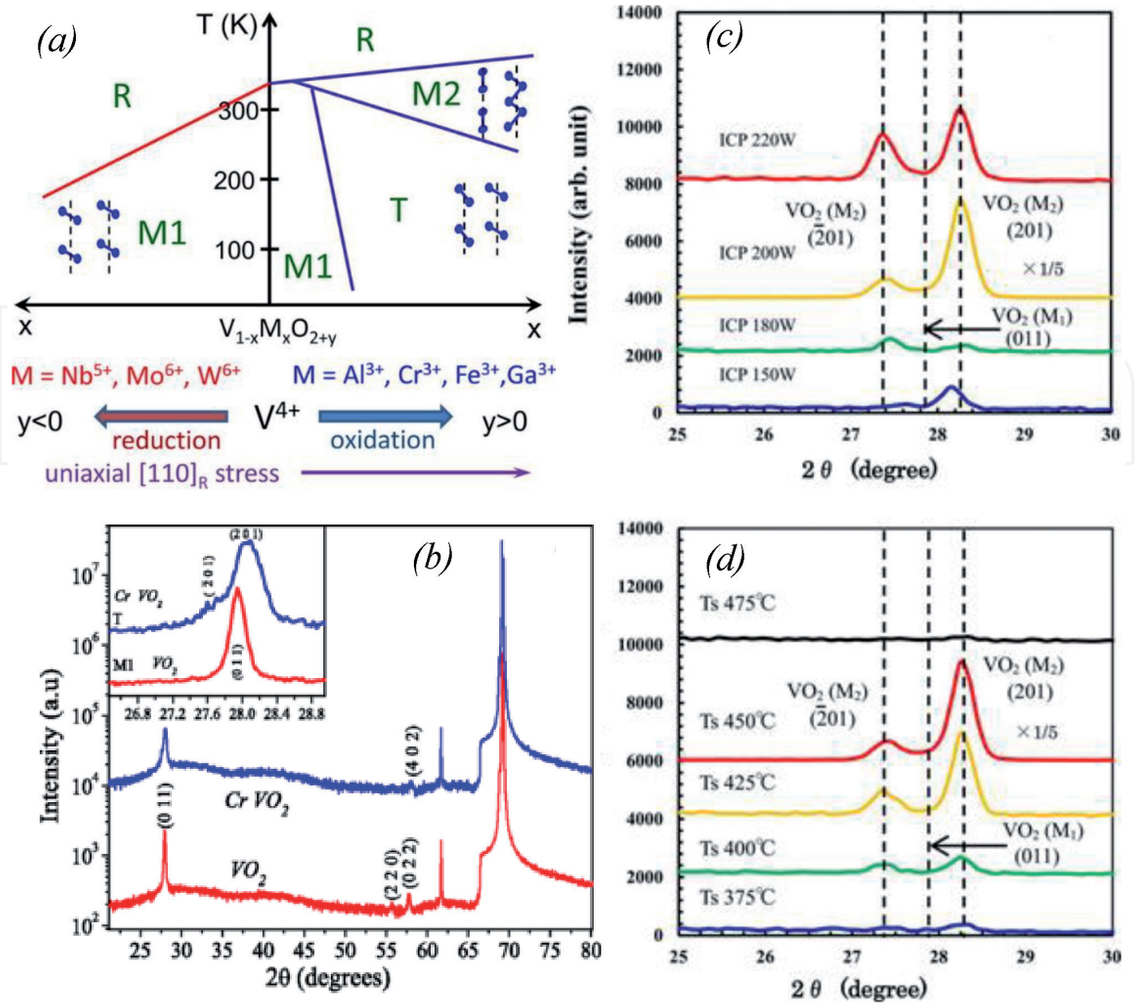

Figure 5.
(a) A temperature-composition phase diagram of VO_2, demonstrating the influence of chemical doping and uniaxial stress on the phase structure of VO_2 (reprinted with permission from Strelcov et al. [35]. Copyright 2012 American Chemical Society). (b), room-temperature XRD patterns of the pure (M1 phase) and Cr-doped (T phase) VO_2 thin films on the [001] Si substrate (adapted from Ref. [15]). (c and d) XRD patterns of the VO_2 films grown on quartz substrates with various RFpower fed to the coil for ICP, at constant Ts of 450°C and at varying Ts, under constant RF power (Reprinted from Ref. [77], with the permission of AIP Publishing).

Recently; several reports are focused on VO_2 (A) and VO_2 (B) phases in the form of bulk and nano-powders where annealing treatment causes them to revert to stable VO_2 (M_1) phase [25]. Chen et al. appears to be the first to report the growth of textured VO_2 (B) films with thickness only <25 nm on $SrTiO_3$ (001) substrate [87].

The good mathing of the a – b plane of VO_2 (B) to that of (001)-oriented perovskites enables the epitaxial growth of phase-pure VO_2 (B) thin films on perovskite substrates, such as $SrTiO_3$ and $LaAlO_3$. Srivastava et al. successfully stablized the single phase VO_2 (B) and VO_2 (A) thin films by tuning the laser retation rate and oxygen partical pressure during PLD while keeping the constant substrate tempearture (T_s = 500°C) [23]. The XRD pattern of their grown films and the phase digram of used deposition parameters are shown in **Figure 7(c)** and **(d)** respectively. Lee et al. argued that a proper choice of T_s is crtical among the deposition parameters for the growth of VO_2 (A) and VO_2 (B) phase thin film on perovskite substrates [60]. They found that the thin films of these phases can reproducibly grow at T_s lower than 430°C only (**Figure 8(a)** and **(b)**). Morover, VO_2 (A) phase can also appear as an intermediate phase (**Figure 8(c)**) when annealing is carried out for VO_2 (B)➔ VO_2 (R) conversion [60]. Wong et al. successfully synthesize thin

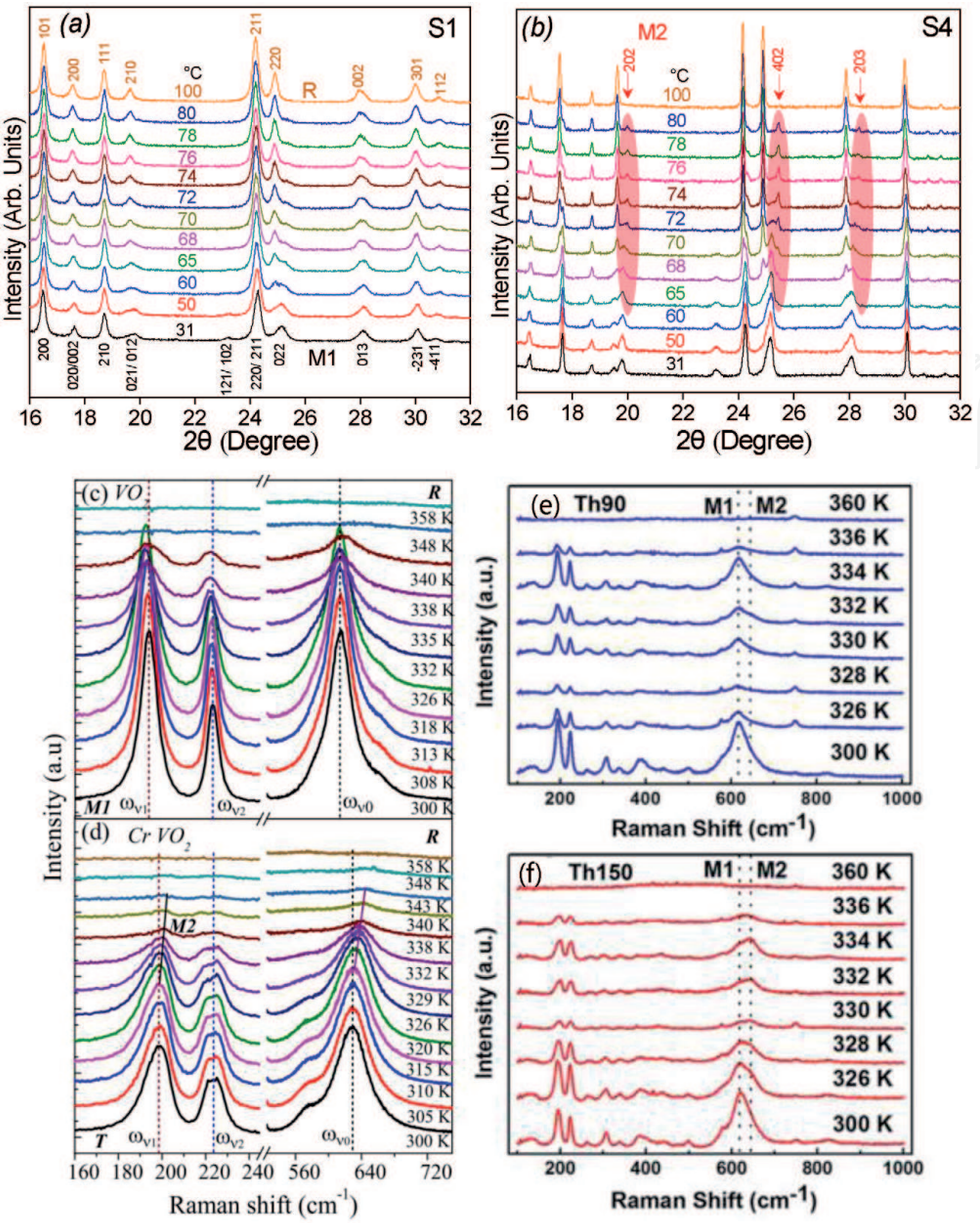

Figure 6.
Temperature dependence of XRD data (at X-ray wavelength (λ) = 0.0693 nm) during heating cycle for VO_2 thin film annealed at (a) 500°C and (b) 530°C (a,b adopted from Ref. [69]). Temperature-dependent Raman spectra of (c) pure and (d) Cr-doped VO_2 thin films collected in the cooling cycles (c, d adopted from Ref. [15]). Temperature dependent Raman spectra of (e) 90 nm and (f) 150 nm thick VO_2 thin film grown on Al_2O_3 substrate (e, f adopted from Ref. [78]).

films of the metastable VO_2 (B) polymorph on (001) $LaAlO_3$ at deposition temperature T_s = 325°C (**Figure 8(d)**) [70]. Very recently, Choi et al. grown epitaxial VO_2 (A) and VO_2 (B) thin films having tungsten doping were grown on (011)-oriented $SrTiO_3$ and 001)-oriented $LaAlO_3$ substrate respectively using PLD [88].

3. Conclusions

An overview of thin film stabilization of different VO_2 polymorphs i.e. VO_2 (M_1), VO_2 (M_2), VO_2 (R), VO_2 (T), VO_2 (A) and VO_2 (B) is presented in this chapter. It is understood that one can stabilize the thin film of a particular VO_2 polymorph by properly selecting the deposition technique, growth parameters, type of substrate and dopant etc.

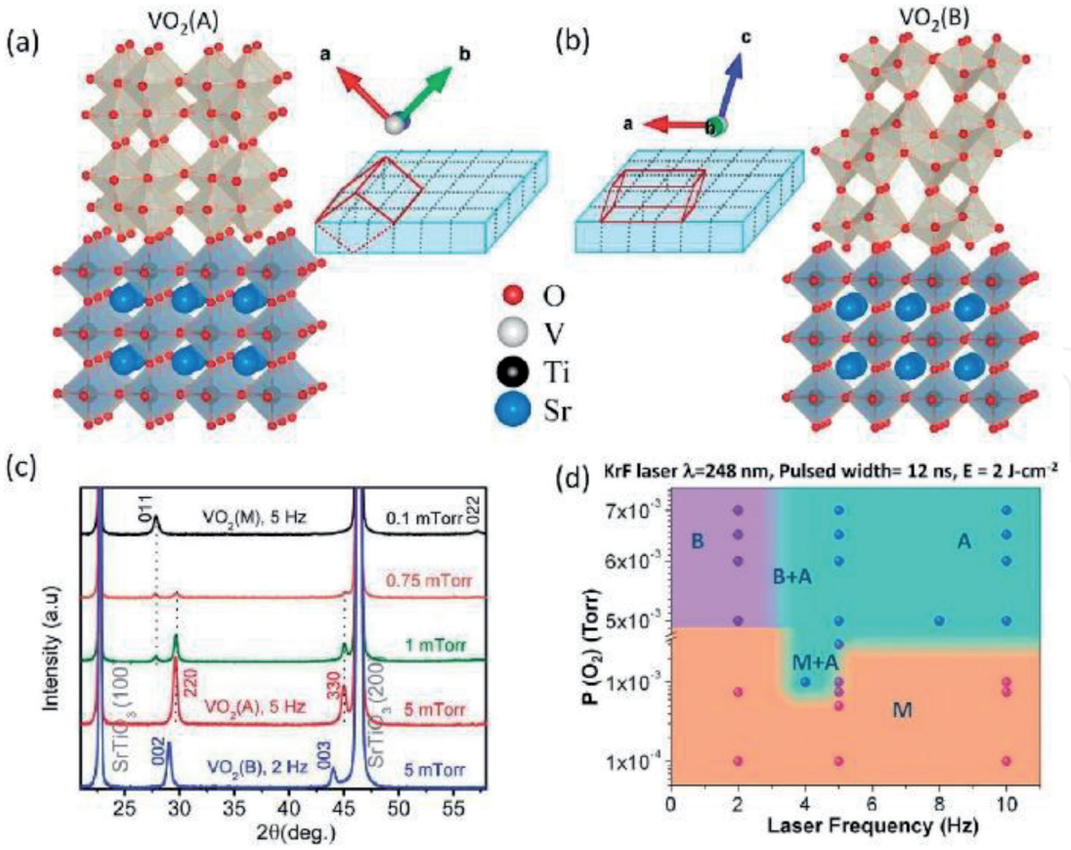

Figure 7.
The schematic crystal structure representation of (a) 220 orientated VO_2 (A), (b) 002 orientated VO_2 (B) grown on $SrTiO_3$ (100) substrate. (c) XRD patterns showing different phases for VO_2 thin films grown at various deposition parameters. (d) Phase diagram showing the role of laser frequency and oxygen pressure during pulsed laser deposition for different polymorphs of VO_2 thin films (a-d adopted from Ref. [23]).

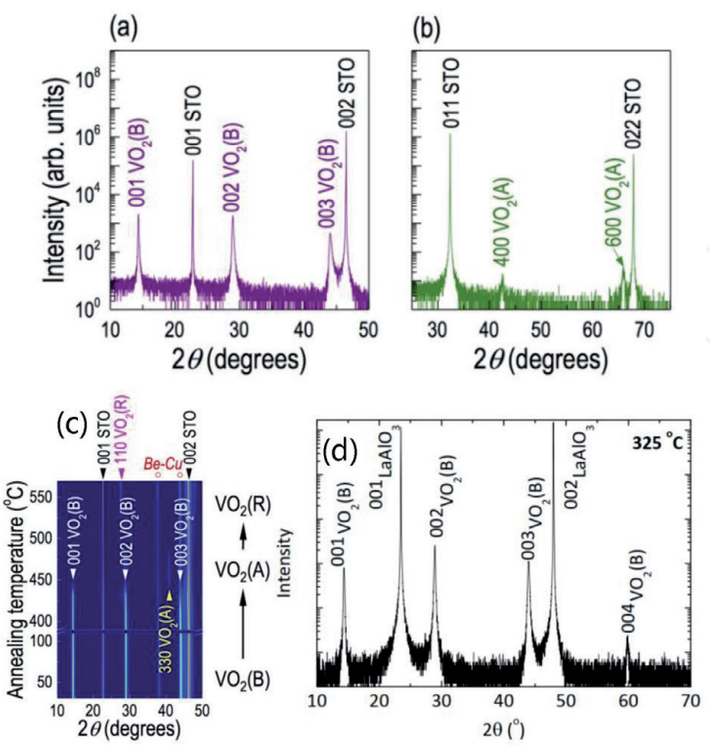

Figure 8.
XRD patterns of (a) VO_2 (B) and (b) VO_2 (A) thin film on $SrTiO_3$ (001) and (011) substrates respectively. (c) XRD during annealing of VO_2 (B)/STO sample (a-c adopted from Ref. [60]). (d) XRD scan of VO_2 (B) film grown on $LaAlO_3$ (001) substrate (adopted from Ref. [70]).

Acknowledgements

This work was supported by National Research Foundation of Korea (NRF) grant (Grant No. NRF-2015R1A5A1009962 and NRF-2019K1A3A7A09033398) funded by the Korean government. Authors also acknowledge the support from Pohang Accelerator Lab in Korea.

Conflict of interest

The authors declare no conflict of interest.

Notes/thanks/other declarations

Authors are thankful to the publisher for waive off the article processing charges of the chapter.

Author details

Manish Kumar[1*], Chirag Saharan[2] and Sunita Rani[1]

1 Pohang Accelerator Laboratory, Pohang University of Science and Technology, Pohang, 37673, South Korea

2 Department of Physics, Deenbandhu Chhotu Ram University of Science and Technology, Murthal, Sonepat (Haryana) - 131039, India

*Address all correspondence to: manish@postech.ac.kr

References

[1] Shahinpoor M, editor. Fundamentals of Smart Materials. 1st ed. Cambridge; Royal Society of Chemistry; 2020.338 p. ISBN: 9781782626459

[2] Kumar M, Phase DM, Choudhary RJ, Lee HH. Structure and functionalities of manganite/cuprate thin film. Current Applied Physics. 2018;**18S**:33-36. DOI: 10.1016/j.cap.2017.11.009

[3] Kumar M, Choudhary RJ, Shukla DK, Phase DM. Metastable magnetic state and magnetotransport in disordered manganite thin film. Journal of Applied Physics. 2014;**115**:163904. DOI: 10.1063/1.4873300

[4] Dagotto E. Complexity in strongly correlated electronic systems. Science. 2005;**309**:257. DOI: 10.1126/science.1107559

[5] Kumar M, Choudhary RJ, Phase DM. Valence band structure of $YMnO_3$ and the spin orbit coupling. Applied Physics Letters. 2013;**102**:182902. DOI: 10.1063/1.4804618

[6] Kumar M, Choudhary RJ, Phase DM. Magnetic and electronic properties of $La_{0.7}Ca_{0.3}MnO_3$/h-$YMnO_3$ bilayer. Journal of Vacuum Science and Technology A. 2016;**34**:021506. DOI: 10.1116/1.4937356

[7] Panchal G, Choudhary RJ, Kumar M, Phase DM. Interfacial spin glass mediated spontaneous exchange bias effect in self-assembled $La_{0.7}Sr_{0.3}MnO_3$: NiO nanocomposite thin films. J. Alloy. Compd. 2019;**796**:196-202. DOI: 10.1016/j.jallcom.2019.05.033

[8] Kumar M, Phase DM, Choudhary RJ. Structural, ferroelectric and dielectric properties of multiferroic $YMnO_3$ synthesized via microwave assisted radiant hybrid sintering. Heliyon. 2019;**4**:e01691. DOI: 10.1016/j.heliyon.2019.e01691

[9] Kumar M, Phase DM, Choudhary RJ, Upadhayay SK, Reddy VR. Microwave assisted radiant hybrid sintering of $YMnO_3$ ceramic: Reduction of microcracking and leakage current. Ceramics International. 2018;**44**:8196. DOI: 10.1016/j.ceramint.2018.01.268

[10] Kumar M, Choudhary RJ, Phase DM. Metastable magnetic state and exchange bias training effect in Mn-rich $YMnO_3$ thin films. Journal of Physics D: Applied Physics. 2015;**48**:125003. DOI: 10.1088/0022-3727/48/12/125003

[11] Kumar M, Choudhary RJ, Shukla DK, Phase DM. Superspin glassy behaviour of $La_{0.7}Ca_{0.3}Mn_{0.85}Al_{0.15}O_3$ thin film. Journal of Applied Physics. 2014;**116**:033917. DOI: 10.1063/1.4890507

[12] Kumar M, Choudhary RJ, Phase DM. Structural and multiferroic properties of self-doped yttrium manganites $YMn_{1+X}O_3$. AIP Conf. Proc. 2015;**1661**:07005. DOI: 10.1063/1.4915383

[13] Devi V, Kumar M, Wadikar AD, Choudhary RJ, Phase DM, Joshi BC. Electronic and multiferroic properties of $Zn0_{.85}Mg_{0.15}O$ thin film. AIP Conf. Proc. 2015;**1665**:080065. DOI: 10.1063/1.4917969

[14] Morin FJ. Oxides which show a metal-to-insulator transition at the neel temperature. Physical Review Letters. 1959;**3**:34. DOI: 10.1103/PhysRevLett.3.34

[15] Majid SS, Shukla DK, Rahman F, Khan S, Gautam K, Ahad A, et al. Insulator-metal transitions in the T phase Cr doped and M1 phase undoped VO_2 thin films. Physical Review B. 2018;**98**:075152. DOI: 10.1103/PhysRevB.98.075152

[16] Liu K, Lee S, Yang S, Delaire O, Wu J. Recent progresses on physics and applications of vanadium dioxide. Materials Today. 2018;**21**:875. DOI: 10.1016/j.mattod.2018.03.029

[17] Yang Z, Ko C, Ramanathan S. Oxide electronics utilizing ultrafast metal-insulator transitions. Annual Review of Materials Research. 2011;**41**:337. DOI: 10.1146/annurev-matsci-062910-100347

[18] Zhou Y, Ramanathan S. Mott memory and neuromorphic devices. Proceedings of the IEEE. 2015;**103**:1289. DOI: 10.1109/jproc.2015.2431914

[19] Shao Z, Cao X, Luo H, Jin P. Recent progress in the phase-transition mechanism and modulation of vanadium dioxide materials. NPG Asia Materials. 2018;**10**:581. DOI: 10.1038/s41427-018-0061-2

[20] Haverkort MW, Hu Z, Tanaka A, Reichelt W, Streltsov SV, Korotin MA, et al. Orbital-assisted metal-insulator transition in VO_2. Physical Review Letters. 2015;**95**:196404. DOI: 10.1103/PhysRevLett.95.196404

[21] O'Callahan BT, Jones AC, Park JH, Cobden DH, Atkin JM, Raschke MB. Inhomogeneity of the ultrafast insulator-to-metal transition dynamics of VO2. Nature Communications. 2015;**6**:6849. DOI: 10.1038/ncomms7849

[22] Gray AX, Jeong J, Aetukuri NP, Granitzka Chen PZ, Kukreja R, Higley D, et al. Correlation-driven insulator-metal transition in near-ideal vanadium dioxide films. Physical Review Letters. 2016;**116**:1. DOI: 10.1103/PhysRevLett.116.116403

[23] Srivastava A, Rotella H, Saha S, Pal B, Kalon G, Mathew S, et al. Selective growth of single phase VO_2(A, B, and M) polymorph thin films. APL Materials. 2015;**3**:026101. DOI: 10.1063/1.4906880

[24] Hagrman D, Zubieta J, Warren CJ, Linda MM, Michael MJT, Robert CH. A new polymorph of VO_2 prepared by soft chemical methods. Journal of Solid State Chemistry. 1998;**138**:178. DOI: 10.1006/jssc.1997.7575

[25] Li M, Magdassi S, Gao Y, Long Y. Hydrothermal synthesis of VO_2 polymorphs: Advantages, challenges and prospects for the application of energy efficient smart windows. Small. 2017;**13**:1701147. DOI: 10.1002/smll.201701147

[26] Liu L, Cao F, Yao T, Xu Y, Zhou M, Qu B, et al. New-phase VO_2 micro/nanostructures: Investigation of phase transformation and magnetic property. New Journal of Chemistry. 2012;**36**:619. DOI: 10.1039/c1nj20798a

[27] Song ZD, Zhang LM, Xia F, Webster N, Song J, Liu B, et al. Controllable synthesis of VO_2(D) and their conversion to VO_2(M) nanostructures with thermochromic phase transition properties. Inorganic Chemistry Frontiers. 2016;**3**:1035. DOI: 10.1039/C6QI00102E

[28] Wu C, Hu Z, Wang W, Zhang M, Yang J, Xie Y. Synthetic paramontroseite VO_2 with good aqueous lithium–ion battery performance. Chemical Communications. 2008;(33):3891. DOI: 10.1039/B806009F

[29] Braham E, Andrews JL, Alivio TEG, Fleer NA, Banerjee S. Stabilization of a metastable tunnel-structured orthorhombic phase of VO_2 upon iridium doping. Phys. Status Solidi A-Appl. Mat. 2018;**215**:1700884. DOI: 10.1002/pssa.201700884

[30] Park JH, Coy JM, Kasirga TS, Huang C, Fei Z, Hunter S, et al. Measurement of a solid-state triple point at the metal–insulator transition in VO_2. Nature. 2013;**500**:431. DOI: 10.1038/nature12425

[31] Galy J, Miehe G. Ab initio structures of (M2) and (M3) VO2 high pressure phases. Solid State Sciences. 1999;**1**:433. DOI: 10.1016/S1293-2558(00)80096-5

[32] Katzke H, Toledano P, Depmeier W. Physical Review B. 2003;**68**:024109. DOI: 10.1103/PhysRevB.68.024109

[33] MacChesney JB, Potter JF, Guggenheim HJ. Preparation and properties of vanadium dioxide films. Journal of the Electrochemical Society. 1968;**115**:52. DOI: 10.1149/1.2411002

[34] Kumar M, Singh JP, Chae KW, Park J, Lee HH. Annealing effect on phase transition and thermochromic properties of VO_2 thin films. Superlattices and Microstructures. 2020;**137**:106335. DOI: 10.1016/j.spmi.2019.106335

[35] Strelcov E, Tselev A, Ivanov I, Budai JD, Zhang J, Tischler JZ, et al. Doping-based stabilization of the M2 phase in free-standing VO_2 nanostructures at room temperature. Nano Letters. 2012;**12**:6198. DOI: 10.1021/nl303065h

[36] Sahana MB, Dharmaprakash MS, Shivashankar SA. Microstructure and properties of VO_2 thin films deposited by MOCVD from vanadyl acetylacetonate. Journal of Materials Chemistry. 2002;**12**:333. DOI: 10.1039/b106563g

[37] Warwick MEA, Binions R. Chemical vapour deposition of thermochromic vanadium dioxide thin films for energy efficient glazing. Journal of Solid State Chemistry. 2014;**214**:53. DOI: 10.1016/j.jssc.2013.10.040

[38] Seyfouri MM, Binions R. Sol-gel approaches to thermochromic vanadium dioxide coating for smart glazing application. Solar Energy Materials & Solar Cells. 2017;**159**:52. DOI: 10.1016/j.solmat.2016.08.035

[39] Koide S, Takei H. Epitaxial growth of VO2 single crystals and their anisotropic properties in electrical resistivities. Journal of the Physical Society of Japan. 1967;**22**:946. DOI: 10.1143/JPSJ.22.946

[40] Fuls EN, Hensler DH, Ross AR. Reactively sputtered vanadium dioxide thin films. Applied Physics Letters. 1967;**10**:199. DOI: 10.1063/1.1754909

[41] Borek M, Qian F, Nagabushnam V, Singh RK. Pulsed-laser deposition of oriented VO_2 thin films on R-cut sapphire substrates. Applied Physics Letters. 1993;**63**:3288. DOI: 10.1063/1.110177

[42] Manish K, Rani S, Lee HH. Thermochromic VO_2 thin films: Growth and characterization. AIP Conf. Proc. 2019;**2142**:080007. DOI: 10.1063/1.5122435

[43] Kumar M, Rani S, Lee HH. Effect of Ti:ZnO layer on the phase transition and optical properties of VO_2 film. Journal of the Korean Physical Society. 2019;**75**:519-522. DOI: 10.3938/jkps.75.519

[44] Kim DH, Kwok HS. Pulsed laser deposition of VO_2 thin films. Applied Physics Letters. 1994;**65**:3188. DOI: 10.1063/1.112476

[45] Émond N, Hendaoui A, Ibrahim A, Al-Naib I, Ozaki T, Chaker M. Transmission of reactive pulsed laser deposited VO_2 films in the THz domain. Applied Surface Science. 2016;**379**:377. DOI: 10.1016/j.apsusc.2016.04.018

[46] Jeong J, Aetukuri NB, Passarello D, Conradson SD, Samant MG. Parkin. Giant reversible, facet-dependent, structural changes in a correlated-electron insulator induced by ionic liquid gating. SSP. PNAS. 2015;**112**:1013. DOI: 10.1073/pnas.1419051112

[47] Kumar M, Choudhary RJ, Phase DM. Growth of different phases of yttrium manganese oxide thin films by pulsed laser deposition. AIP Conf. Proc. 2012;**1447**:655. DOI: 10.1063/1.4710173

[48] Devi V, Joshi BC, Kumar M, Choudhary RJ. Structural and optical properties of Cd and Mg doped zinc oxide thin films deposited by pulsed laser deposition. Journal of Physics: Conference Series. 2014;**534**:012047. DOI: 10.1088/1742-6596/534/1/012047

[49] Devi V, Kumar M, Kumar R, Joshi BC. Effect of substrate temperature and oxygen partial pressure on structural and optical properties of Mg doped ZnO thin films. Ceramics International. 2015;**41**:6269. DOI: 10.1016/j.ceramint.2015.01.049

[50] Devi V, Kumar M, Shukla DK, Choudhary RJ, Phase DM, Kumar R, et al. Structural, optical and electronic structure studies of Al doped ZnO thin films. Superlattices and Microstructures. 2015;**83**:431. DOI: 10.1016/j.spmi.2015.03.047

[51] Devi V, Kumar M, Choudhary RJ, Phase DM, Kumar R, Joshi BC. Band offset studies in pulse laser deposited $Zn_{1-x}Cd_xO$/ZnO hetero-junction. Journal of Applied Physics. 2015;**117**:225305. DOI: 10.1063/1.4922425

[52] Devi V, Kumar M, Kumar R, Singh A, Joshi BC. Band offset measurements in $Zn_{1-x}Sb_xO$/ZnO hetero-junctions. J. Phys. D-Appl. Phys. 2015;**48**:335103. DOI: 10.1088/0022-3727/48/33/335103

[53] Devi V, Pandey H, Tripathi D, Kumar M, Joshi BC. Optical and electrical properties of pristine and Al doped ZnO thin films. AIP Conf. Proc. 2019;**2136**:040010. DOI: 10.1063/1.5120924

[54] Devi V, Kumar M, Choudhary RJ, Joshi BC. Structural and optical properties of $Zn_{1-x}Cd_xO$ thin films. AIP Conf. Proc. 2015;**1661**:110006. DOI: 10.1063/1.4915451

[55] Bhardwaj R, Kaur B, Singh JP, Kumar M, Lee HH, Kumar P, et al. Role of low energy transition metal ions in Interface formation in ZnO thin films and their effect on magnetic properties for Spintronics applications. Applied Surface Science. 2019;**479**:1021. DOI: 10.1016/j.apsusc.2019.02.107

[56] Kumar M, Singh JP, Chae KH, Lee HH. Structural and electronic properties of ZnO and Ti/Mn:ZnO flexible thin films. Journal of the Korean Physical Society. 2020;**77**:452. DOI: 10.3938/jkps.77.452

[57] Singh JP, Kumar M, Lim WC, Lee HH, Lee YM, Lee S, et al. MgO thin film growth on Si(001) by radio-frequency sputtering method. Journal of Nanoscience and Nanotechnology. 2020;**20**:7555. DOI: 10.1166/jnn.2020.18613

[58] Kumar M, Singh JP, Chae KH, Kim JH, Lee HH. Structure, optical and electronic structure studies of Ti:ZnO thin films. J. Alloy. Compd. 2018;**759**:8. DOI: 10.1016/j.jallcom.2018.04.338

[59] Singh JP, Ji MJ, Kumar M, Lee IJ, Chae KH. Unveiling the nature of adsorbed species onto the surface of MgO thin films during prolonged annealing. J. Alloy. Compd. 2018;**748**:355. DOI: 10.1016/j.jallcom.2018.02.344

[60] Lee S, Ivanov IN, Keum JK, Lee HN. Epitaxial stabilization and phase instability of VO_2 polymorphs. Scientific Reports. 2016;**6**:19621. DOI: 10.1038/srep19621

[61] Choi S, Chang SJ, Oh J, Jang HJ, Lee S. Electrical and optical properties of VO2 polymorphic films grown Epitaxially on Y-stabilized ZrO_2. Adv.

Electron. Mater. 2018;**4**:1700620. DOI: 10.1002/aelm.201700620

[62] Chamberland BL. New defect vanadium dioxide phases. Journal of Solid State Chemistry. 1973;**7**:377. DOI: 10.1016/0022-4596(73)90166-7

[63] Ghedira M, Vincent H, Marezio M, Launay JC. Structural aspects of the metal-insulator transitions in V0.985Al0.015O2. Journal of Solid State Chemistry. 1977;**22**:423. DOI: 10.1016/0022-4596(77)90020-2

[64] Basu R, Srihari V, Sardar M, Srivastava SK, Bera S, Dhara S. Probing phase transition in VO_2 with the novel observation of low-frequency collective spin excitation. Scientific Reports. 2020;**10**:1977. DOI: 10.1038/s41598-020-58813-x

[65] Yang TH, Aggarwal R, Gupta A, Zhou H, Narayan RJ, Narayan J. Semiconductor-metal transition characteristics of VO_2 thin films grown on c- and r-sapphire substrates. Journal of Applied Physics. 2010;**107**:053514. DOI: 10.1063/1.3327241

[66] Wong FJ, Zhou Y, Ramanathan S. Epitaxial variants of VO_2 thin films on complex oxide single crystal substrates with 3m surface symmetry. Journal of Crystal Growth. 2013;**364**:74. DOI: 10.1016/j.jcrysgro.2012.11.054

[67] Zhang H, Zhang L, Mukherjee D, Zheng Y, Haislmaier R, Alem N, et al. Wafer-scale growth of VO2 thin films using a combinatorial approach. Nature Communications. 2015;**6**:8475. DOI: 10.1038/ncomms9475

[68] Shao Z, Wang L, Chang T, Xu F, Sun G, Jin P, et al. Controllable phase-transition temperature upon strain release in VO_2/MgF_2 epitaxial films. Journal of Applied Physics. 2020;**128**:045303. DOI: 10.1063/5.0011423

[69] Kumar M, Rani S, Singh JP, Chae KW, Kim Y, Park J, et al. Structural phase control and thermochromic modulation of VO2 thin films by post thermal annealing. Applied Surface Science. 2020;**529**:147093. DOI: 10.1016/j.apsusc.2020.147093

[70] Wong FJ, Ramanathan S. Synthesis of epitaxial rutile-type VO_2 and VO_2 (B) polymorph films. Proc. of SPIE. 2014;**8987**:89870W. DOI: 10.1117/12.2044055

[71] Fan LL, Chen S, Luo ZL, Liu QH, Wu YF, Song L, et al. Strain dynamics of ultrathin VO2 film grown on TiO2 (001) and the associated phase transition modulation. Nano Letters. 2014;**14**:4036. DOI: 10.1021/nl501480f

[72] Zhao Y, Karaoglan-Bebek G, Pan X, Holtz M, Bernussi AA, Fan Z. Hydrogen-doping stabilized metallic VO2 (R) thin films and their application to suppress Fabry-Perot resonances in the terahertz regime. Applied Physics Letters. 2014;**104**:241901. DOI: 10.1063/1.4884077

[73] Liang YG, Lee S, Yu HS, Zhang HR, Liang YJ, Zavalij PY, et al. Tuning the hysteresis of a metal-insulator transition via lattice compatibility. Nature Communications. 2020;**11**:3539. DOI: 10.1038/s41467-020-17351-w

[74] Yoon H, Choi M, Lim T, Kwon H, Ihm K, Kim J, et al. Reversible phase modulation and hydrogen storage in multivalent VO_2 epitaxial thin films. Nature Materials. 2016;**15**:1113. DOI: 10.1038/nmat4692

[75] Lee D, Kim H, Kim JW, Lee IJ, Kim Y, Yun H, et al. Hydrogen incorporation induced the octahedral symmetry variation in VO_2 films. Applied Surface Science. 2017;**396**:36. DOI: 10.1016/j.apsusc.2016.11.047

[76] Jeong J, Aetukuri N, Graf T, Schladt TD, Samant MG, Parkin SSP.

Suppression of metal-insulator transition in VO_2 by electric field-induced oxygen vacancy formation. Science. 2013;**339**:1402. DOI: 10.1126/science.1230512

[77] Okimura K, Watanabe T, Sakai J. Stress-induced VO_2 films with M_2 monoclinic phase stable at room temperature grown by inductively coupled plasma-assisted reactive sputtering. Journal of Applied Physics. 2012;**111**:073514. DOI: 10.1063/1.3700210

[78] Ji Y, Zhang Y, Gao M, Yuan Z, Xia Y, Jin C, et al. Role of microstructures on the M1-M2 phase transition in epitaxial VO_2 thin films. Scientific Reports. 2014;**4**:4854. DOI: 10.1038/srep04854

[79] Azhan NH, Su K, Okimura K, Zaghrioui M, Sakai J. Appearance of large crystalline domains in VO_2 films grown on sapphire (001) and their phase transition characteristics. Journal of Applied Physics. 2015;**117**:245314. DOI: 10.1063/1.4923223

[80] Sharma Y, Holt MV, Laanait N, Gao X, Ivanov IN, Collins L, et al. Competing phases in epitaxial vanadium dioxide at nanoscale. APL Materials. 2019;**7**:081127. DOI: 10.1063/1.5115784

[81] Pouget JP, Launois H, D'Haenens JP, Merenda P, Rice TM. Electron localization induced by uniaxial stress in pure VO_2. Physical Review Letters. 1975;**35**:873. DOI: 10.1103/PhysRevLett.35.873

[82] Li W, Dahn JR, Wainwright DS. Rechargeable lithium batteries with aqueous electrolytes. Science. 1994;**264**:1115. DOI: 10.1126/science.264.5162.1115

[83] Lee S, Sun XG, Lubimtsev AA, Gao X, Ganesh P, Ward TZ, et al. Persistent electrochemical performance in epitaxial VO_2 (B). Nano Letters. 2017;**17**:2229. DOI: 10.1021/acs.nanolett.6b04831

[84] Xia C, Lin Z, Zhou Y, Zhao C, Liang H, Rozier P, et al. Large intercalation Pseudocapacitance in 2D VO2(B): Breaking through the kinetic barrier. Adv. Mat. 2018;**30**:1803594. DOI: 10.1002/adma.201803594

[85] Oka Y, Sato S, Yao T, Yamamoto N. Crystal structures and transition mechanism of VO_2 (a). Journal of Solid State Chemistry. 1998;**141**:594. DOI: 10.1006/jssc.1998.8025

[86] Zhang S, Shang B, Yang J, Yan W, Wei S, Xie Y. From VO_2 (B) to VO_2 (a) nanobelts: First hydrothermal transformation, spectroscopic study and first principles calculation. Physical Chemistry Chemical Physics. 2011;**13**:15873. DOI: 10.1039/C1CP20838A

[87] Chen A, Bi Z, Zhang W, Jian J, Jia QX, Wang H. Textured metastable VO_2 (B) thin films on $SrTiO_3$ substrates with significantly enhanced conductivity. Applied Physics Letters. 2014;**104**:071909. DOI: 10.1063/1.4865898

[88] Choi S, Ahn G, Moon SJ, Lee S. Tunable resistivity of correlated VO_2(A) and VO_2(B) via tungsten doping. Scientific Reports. 2020;**10**:9721. DOI: 10.1038/s41598-020-66439-2